Determining the Pareto front of distributed generator and static VAR compensator units placement in distribution networks

Bahman Ahmadi, Ramazan Çağlar
Department of Electrical Engineering, Istanbul Technical University, Istanbul, Turkey

Article Info

ABSTRACT

The integration of distributed generators (DGs), which are based on renewable energy sources, energy storage systems, and static VAR compensators (SVCs), requires considering more challenging operational cases due to the variability of DG production contributed by different characteristics for different time sequences. The size, quantity, technology, and location of DG units have major effects on the system to benefit from the integration. All these aspects create a multi-objective scope; therefore, it is considered a multi-objective mixed-integer optimization problem. This paper presents an improved multi-objective salp swarm optimization algorithm (MOSSA) to obtain multiple Pareto efficient solutions for the optimal number, location, and capacity of DGs and the controlling strategy of SVC a radial distribution system. MOSSA is a bio-inspired optimizer based on swarm intelligence techniques and it is used in finding the optimal solution for a global optimization problem. Two sets of objective functions have been formulated minimizing DGs and SVC cost, voltage violation, energy losses, and system emission cost. The usefulness of the proposed MOSSA has been tested with the 33-bus and 141-bus radial distribution systems and the qualitative comparisons against two well-known algorithms, multiple objective evolutionary algorithms based on decomposition (MOEA/D), and multiple objective particle swarm optimization (MOPSO) algorithm.
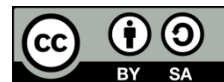
Corresponding Author:

Bahman Ahmadi
Department of Electrical Engineering, Istanbul Technical University
Istanbul, Turkey
Email: ahmadi18@itu.edu.tr, caglarr@itu.edu.tr

1. INTRODUCTION

With the growing penetration of small-scale distributed generation (DG) technology and static VAR compensator (SVC) units in the distribution systems, the usage of these units has become a hot research topic for researchers. In general, the mentioned units are used for improving the power network benefits. The location, size, and operation planning of DGs and SVCs need to be designed and planned optimally to find optimal solutions that provide the benefits of the unit and the optimal economic point of view [1], [2]. Many available objectives and constraint factors considered being optimally minimized or maximized. From the perspective of mathematical optimization, DG and SVC units sizing, siting, and planning are complex multi-objective optimization problems in the distribution system, so many papers optimized single [3], [4] or multi objectives [5]–[7] among available objective functions using either analytic or heuristic methods. The multi-objective salp swarm algorithm (MOSSA) afforded a robust searching capability in multi-objective components to get the most proximate Pareto optimal solutions among various techniques and tools.

Different factors such as technical and environmental concerns, increasing purchasing of energy, and restructuring electricity markets become the reason for the growth of DG units' penetration in the microgrids. Although appropriate usage of DG units in the system will result in several benefits for both utility and DG owners such as increasing power quality [8], reducing the greenhouse gases, losses minimization [9], and reliability improvement, but improper incorporation of DG units into the distribution networks may cause serious security problems [10]. The SVC units have been used to improve the system's overall power quality by simultaneous control actions [11]. By optimal allocating these units together with DG units, they can provide all the mentioned advantages to the system.

In the classical multi-objective optimization method, multiple-objective optimization problems were objective functions formulated as a weighted sum of all objective functions using proper weighting factors. By changing these weight factors, finally, the Pareto optimal solutions were obtained. Several multi-objective optimization algorithms are developed to automatically handle the problem and find trade-off solutions because of the motioned problems. In study [10], DG owner profit and system cost were optimized for optimal allocation of small scaled DG units and system reconfiguration problems. In study [12], multi-objective mixture teaching-learning based on the grey wolf optimizer algorithm method used to find Pareto solution to minimize power losses and improve the system's reliability. Multiple-objective particle swarm optimization (MOPSO) was used for allocating multi-type DGs and battery banks in [13]. The best type, location size of distributed generations, SVC, tap changers, and energy storage systems find while minimizing the system voltage deviation [14]. The krill herd algorithm (KHA) was used to minimize the power losses while finding optimal DG allocation [15].

The location of DG units in the radial distribution system optimally found using a multi-objective algorithm based on a chaotic differential evolution (MOCDE) algorithm [16]. The multi-objectives such as voltage violation, yearly loss and DG costs, and power losses were used to find all the Pareto optimal solutions. In studies [17], [18], the wind turbines (WTs) and hybrid energy storage system (HESS) units size optimally found using a single-objective optimization algorithm such as genetic and grey wolf algorithms. In study [19], the size of multi-type DG units found by water irrigation using genetic algorithm for improving the DG owner and utility benefits. The SVC units in [20] used to improve the systems' voltage stability index. Aiming to minimize thermal power plant gas pollution was one of the objectives in [21]. Among those various paper research still, there is a gap in finding the Pareto optimal solution of optimal site, size, type, number, and operation of DG and SVC units.

In this paper, two sets of objective functions, including voltage violation, total energy loss, costs of DG and SVC units, and thermal power plant emission costs, are considered main objectives. Multiple types of DG units modeled as negative load using real wind speed and sun irradiation data. The SVC units are considered and modeled to help DG units to improve the system's power quality. Four different types of loads (commercial, residential, industrial, and mixed load models) are considered in this paper. The proposed MOSSA algorithm is applied to find the near-optimal solutions of the best number, site, and sizing of the DGs and SVC and SVC control strategy.

The feasibility of the prepared technique was tested on both IEEE 33-bus network and 141-bus radial distribution network. The results are compared with well-known algorithms referred to as multi-objective particle swarm optimization (MOPSO) algorithm and multi-objective evolutionary algorithms based on decomposition (MOEA/D) algorithms. To showing the better quality of Pareto front solutions obtained by proposed MOSSA compared to the classical optimization methods, the spacing metric (S-metric) and comparison metric (C-metric) considered and compared with a box plot. The main contributions of this work explained in the following points:
  a. The MOSSA is presented and implemented with proposed sets of multiple-objectives for finding optimal operation strategy, number, size, location, and type of DGs and SVCs.
  b. The optimal Pareto front solutions determined for four different study cases, including installing photovoltaic (PV) generation units, installing WT units, installing PV and WT units, and installing multi-type DG and SVC units.
  c. The Pareto optimal solution obtained for different scenario load modeling cases.
  d. The quality of Pareto solutions determines by make a results comparison to the MOPSO and MOEA/D algorithms result for 20 runs using the C and spacing metrics.

The structural organization of the paper is as follows. The MOSSA method and objectives formulation proposed in section 2, then section 3 is devoted to DG and SVC units, and test system modeling. Section 4 shows the simulation results and comparing the quality of the results for test system applications. Finally, conclusion is given in section 5.

2.   MOSSA CONCEPT AND OBJECTIVE MODEL
2.1. Multiple objectives optimization concept overview
Multi-objective optimization formulation can be written as a minimization problem as (1).

$$\underset{w.r.t\ x}{Minimize}\ F(x) = \{f_1(x), f_2(x), \dots, f_n(x)\} \tag{1}$$

$$Subject\ to: \begin{cases} G_i(x) \geq 0, & i = 1, 2, 3, \dots, p \\ H_i(x) = 0, & i = 1, 2, 3, \dots, m \\ lb_i \leq x_i \leq ub_i, i = 1, 2, 3, \dots, d \end{cases}$$

where x is the positions of the solution and the term n represents the number of proposed objectives, p, and m in G_i and H_i represent the number of existed equality equations and the inequality constraints, and d is the number of dimension (variables) between lb and ub values, respectively. Pareto optimal dominance method used to determine the near-optimal Paretos [22]. A set of Pareto optimal solutions for each group of multi-objective problems describes the best trade-offs between the multi-objectives. In multi-objective optimization, a solution is better than another (dominate it) if it has the same and at least a better value in one of the objectives. If this fact does not hold between two solutions, we called these two solutions, Pareto optimal (non-dominated solutions).

2.2. Inspiration, mathematical model of MOSSA
The MOSSA is presented by Mirjalili *et al.* in 2017 [23] regarding the swarming social behavior of the salps. These species are part of the family of *Salpidae*; their body is very same as jellyfish. Salps used their body to pump the water for movement.

In the MOSSA modeling, the behavior of salps to better movement and food-seeking are the mimic. The population of salps is divided into two groups: leader and followers. Usually, the leaders manage the group, and the followers obey the leader either directly or by following the followers indirectly. The salps position is updated by (2) and (3):

$$S_j^1 : \begin{cases} r_1\left(\left(ub_j - lb_j\right) \times r_2 + lb_j\right) - F_j, & r_3 \geq 0.5 \\ r_1\left(\left(ub_j - lb_j\right) \times r_2 + lb_j\right) + F_j, & r_3 < 0.5 \end{cases} \tag{2}$$

$$r_1 = 2e^{-R}, \quad R = \left(\frac{4l}{L}\right)^2 \tag{3}$$

where S_j^1 refers to the jth salp leader position with d dimensions, F_j is the food source's position in the j variable. Note that the food position is selected from the Archive repository space. r_2 and r_3 are random numbers between zero to one. The l represents the current iteration number while L is used for the number of maximum iterations, and coefficient r_1 is a parameter that balances the exploration and exploitation phase. Follower salps positions, update using Newton's law of motion and e expressed as (4).

$$S_j^i = 0.5(S_j^i + S_j^{i-1}) \tag{4}$$

where i is a number between 2 and maximum search agent number.

The MOSSA algorithm can use two-stepping criteria. One is setting a maximum iteration number for the main loop of the algorithm. Two for each iteration, the algorithm can stop if the set of Pareto front solutions at the current iteration compared to a predefined iteration before has less than a predefined tolerance different solution.

2.3. Optimization objectives
In this section, we present the formulation of the objectives used for the DGs and SVC units' allocation problem. In (1), the objectives ($\{f_1, f_2, \dots, f_n\}$) chosen from our objective function and x will be site vectors, size vectors and type vectors of DG unit and size vectors and site vectors and operation strategy vectors for SVC units. The formulation for any set of objectives can be written as (5).

$$\underset{w.r.t\ \vec{S}, \vec{L}, \vec{O}}{Minimize\ \{F_1, F_2, F_3\}} \tag{5}$$

where $\vec{S}$, $\vec{L}$, and $\vec{O}$ denoted the sizes the locations, and operation strategy of the DGs and SVC units.

2.3.1. Voltage violation

Voltage violation objective for controlling the system's voltage profile modeled as differences between each bus voltage magnitude with connected busses in the feeder as (6).

$$OF_v = \sum_{i=1}^{N_t} \sum_{j=1}^{N_{NUS}} (|V_j^i - V_{ref}| + KP_{F_1}^i) \tag{6}$$

where N_t represents the total hours of the optimization process (period), N_{NUS} is the total system's node number, and V_j^i is the jth node's voltage magnitude at hour i. The $P_{F_1}^i$ part works as a penalty in the function to find a better solution with minimum number of voltage violations, and K is set dynamically between the 100 to 0 over the term of iteration number at each iteration.

$$P_{F_1}^i = \begin{cases} (V_j^i - 0.95V_{ref})^2, & if\ V_j^i \leq 0.95V_{ref} \\ 0, & if\ 0.95V_{ref} < V_j^i < 1.05V_{ref} \\ (V_j^i - 1.05V_{ref})^2, & if\ V_j^i \geq 1.05V_{ref} \end{cases} \tag{7}$$

2.3.2. Total energy losses in system branches

Real power loss in j^{th} branch from N_{br} branch in the system at time i can be calculated using $Pl_j^i = (I_j^i)^2 . R_j$. Where, R_j is the line resistance of the jth branch. The summation of energy loss of the network is an objective function to be minimized. This objective function formulated as (8).

$$OF_l = \sum_{i=1}^{N_t} \sum_{j=1}^{N_{br}} Pl_j^i \tag{8}$$

2.3.3. Annual costs including operation, investment, and maintenance cost

The annual costs of the WT and PV units include DG unit annualized installation costs and also operation and maintenance costs. For this purpose, the DG units' costs per kW size and expected lifetimes are considered to be the same for different DG units. SVC devices cost modeled as the total investment and infrastructure costs [24]. This objective can represent mathematically as (9)-(13):

$$OF_c = C_{PV} + C_{WT} + C_{SVC} \tag{9}$$

$$C_{PV} = \sum_{n=1}^{N_{PV}} (\overline{IC}_{PV} \times C_{\tau_{PV}} + \overline{OM}_{PV}) \times S_{PV_n} \tag{10}$$

$$C_{WT} = \sum_{n=1}^{N_{WT}} (\overline{IC}_{WT} \times C_{\tau_{WT}} + \overline{OM}_{WT}) \times S_{WT_n} \tag{11}$$

$$C_{SVC} = \sum_{n=1}^{N_{SVC}} (0.0003 S_{SVC_n}^2 - 0.3051 S_{SVC} + 127.38) \tag{12}$$

$$C_{\tau_x} = \frac{r(1+r)^{\tau_x}}{(1+r)^{\tau_x - 1}} \tag{13}$$

where C_{WT} and C_{PV} are the annualized operation, investment, and maintenance cost of WTs and PVs, respectively. DG units' cost is dependent on the total installation size of the units in kW, where SVC costs depend on device size in kVAr. Here $\overline{IC}$ denotes the investment cost of the units in USD/kW or USD/kWh. The term of $\overline{OM}$ denotes the unit's annual operation and maintenance costs of the units in USD/kW-yr or USD/kW h-yr. All the parameters set as the values find at the [25]–[27]. The term τ is the estimated lifetime of the units in years and S represents the size of different DGs. N_{PV}, N_{WT} and N_{SVC} show the number of DG and SVC units, which are determined for each case of study in the optimization process. Finally, an interest rate of r proposed in capacity recovery factor (C_{τ_x}) for DG units.

2.3.4. Thermal power plant emission costs

Global warming has been a primary concern in current years due to the constant rise in greenhouse gas emissions. Greenhouse gases produced by the power plants such as CO_2, CO, SO_2, and NO_x, which are mainly blamed for causing global warming, occupy a high amount of the total emissions. Atmospheric emissions costs of the grid mainly arise due to increasing purchasing electricity from the thermal power plant. The mentioned gases pollution emission cost such as emission intensity (EI) and environmental value

(EV) shown in Table 1 [28]. Annual emission and electricity generated by the main grid generator formulated as (14).

$$OF_e = (\sum_{j=1}^{N_g} K_j \times E_j) \sum_{i=1}^{8760} P_{MG_i} \tag{14}$$

where K_j and E_j are environmental value and emission intensity of jth type of gas and P_{MG_i} shows the generated active power in thermal power plant.

Table 1. The emission intensities and cost of pollution gases

	SO_2	NO_x	CO_2	CO
EI(g/kWh)	6.481	2.884	6239	0.1083
EV($/kg)	0.875	1.25	0.0041	0.145

2.4. Problem constraints

Various inequality and equality constraints considered in this work, such as the system power balance constraint, SVC, PV, and WT unit constraints.
- Power balance

$$S_{MG}^i + S_{PV}^i + S_{WT}^i + S_{SVC}^i - S_{Load}^i - S_l^i = 0, \quad i = 1, 2, \ldots, N_T \tag{15}$$

where S_{MG} is the active and reactive power of the main generator, S_{SVC} shows the absorption\injected reactive power of SVCs. The S_{WT} and S_{PV} are output power(s) of DGs. Active and reactive loads shown by S_{Load}, S_l is active and reactive branch losses at time i, respectively.
- Main grid generation limits

$$S_{MG}^i \le S_{MG_{max}}, \quad i = 1, 2, \ldots, N_T \tag{16}$$

- WT and PV generation limits

$$0.2MW \le S_{PV} \le 1MW \tag{17}$$

$$0.2MW \le S_{WT} \le 1MW \tag{18}$$

total PV and WT size installed at each bus except slack bus cannot exceed 1MW and DG power factor limit set to be 1 in this paper.
- SVC device limits.

$$S_{SVC} \le 1MVAr \tag{19}$$

$$Q_{SVC}^i \le S_{SVC}, \quad i = 1, 2, \ldots, N_T \tag{20}$$

where maximum SVC size set to be 1 MVar and at each time step SVC controller can set SVC to be between zero and SVC unit size.

2.5. MOSSA implementation procedure

Implementation of the proposed objective function into the MOSSA algorithm can be done via the following procedure.
Step 1: Provided the algorithm all the needed input data such as: i) the desired number and outputs for the DG units, ii) sizes and locations restrictions, iii) number of search agents (population), maximum Archive number, and the maximum number of iterations, and iv) test system line and load data.
Step 2: Initialize first solutions (initial units' locations and sizes or SVC operation controls variables) in the ranges of the solution search space randomly concerning constraints.
Step 3: Calculate the objectives with respect to the positions of the search agents and update the solutions stored in archive repository.
Step 4: Update non-dominated solution to Archive repository.
Step 5: Select an archive solution randomly as a food source.

Step 6: Update the salp swarm leader positions, either exploration or exploitation phases concerning food source position.

Step 7: Update the salp swarm followers' positions using (4).

Step 8: Check the boundaries of positions of the new solutions and if they are out of search space boundaries bring them back to space.

Step 9: Check stopping condition of MOSSA by either setting a maximum iteration number or proposed stopping condition and repeat step 3.

3.   DOMAIN NAME SYSTEM (DNS), DISTRIBUTED GENERATOR (DG) AND STATIC VAR COMPENSATORS (SVC) MODELING

3.1. DNS line and load modeling

The IEEE 33-bus system and also 141-bus systems are radial in nature. Feeders' data are taken from [29], [30] papers. The rated powers levels of the load points were used as peak load in the load curve. The 33-bus system peak load is 3.715 MW, and power losses matching to this load point were 201.91 kW. Respectively for the 141-bus system, the peak load was 11.890 MW, and real power losses for this load point was 628.2 kW using forward-backward sweep (FBS) power flow method proposed in [31]. The FBS algorithm is based on Kirchoff's voltage law (KVL) and Kirchoff's current law (KCL), and it is prepared in two significant steps, namely the backward sweep (BS) and the forward sweep (FS). In the backward sweep step, the branch currents are calculated using the KCL method, while in the forward sweep step, the busses voltage is calculated according to KVL. Industrial, residential, commercial [32] and a real data of distribution system with mixed load type [33] model curves have been adopted for the study. This load curves show in Figure 1.
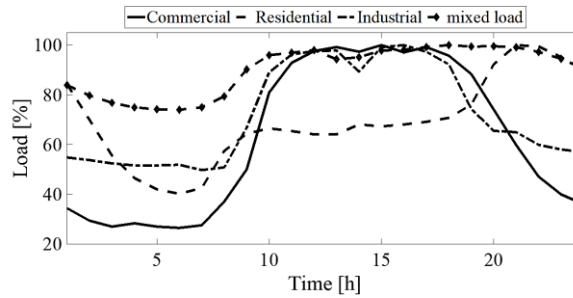

Figure 1. Scaled load demand curves

3.2. DNs line and load modeling

In this paper, the DG unit power factor sets to one and the outputs of DGs are modeled as a negative PQ load. The monthly average values estimated for DGs output using real data of wind speed and sun radiation. The DG units output assumption contains one day with 24-hour period scaled DG output, this data provided in [34], [35]. The monthly time sequence characteristic of PV and WT units are illustrated in Figure 2(a) and 2(b). SVC units installed at each bus as negative reactive power and for each time step the amount of this reactive power can be controlled using SVC controller.
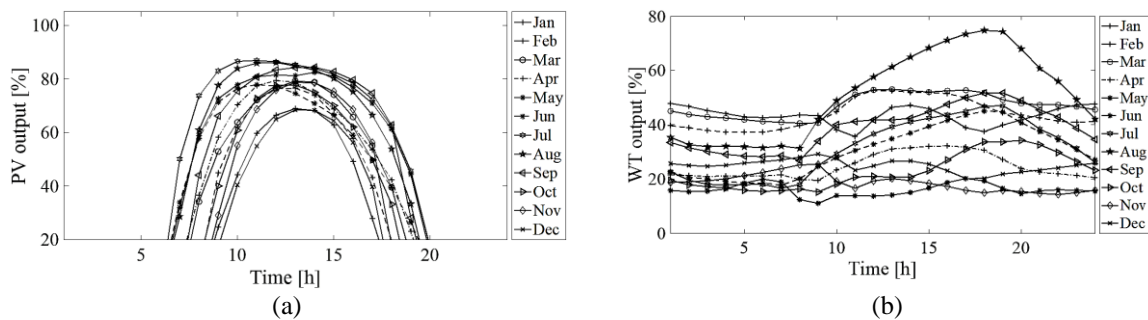

Figure 2. The monthly time sequence characteristic for DG output in (a) PV output and (b) WT output

4. RESULT AND DISCUSSION

4.1. 33-bus system

The optimal DG and SVC units under consideration using MOSSA has been designed and implemented for the different loads and DGs output data provided in the past sections. The MOSSA has been applied to various scenarios such as: Optimal size, number, and location of PV units or WT units, optimal size, number, and location of PV units and WT units, and optimal size, number, and location of PV units, WT units and SVC units. The different load curve characteristic used in proposed scenarios to find out best Pareto fronts of minimizing voltage violation, energy losses and DG units' costs (21) and minimizing voltage violation, thermal generators emission cost, and DG units' costs (22). The minimization problems can formulate as (21), (22):

$$\text{Minimize } \{OF_v, OF_l, OF_c\}$$
$$w.r.t \ \vec{S}, \vec{L}, \vec{O} \tag{21}$$

$$\text{Minimize } \{OF_v, OF_e, OF_c\}$$
$$w.r.t \ \vec{S}, \vec{L}, \vec{O} \tag{22}$$

where OF_l value represent total energy losses in MWh, OF_c value represent total DG and SVC costs in million dollars and OF_e value represent annual emission cost in million dollars.

The optimization algorithm parameters set as 50 for salp population size, 100 for maximum archive size, maximum iteration set as 5000 and MATLAB 2020 used for the simulation on the personal computer with 3.6 GHz i-7 processor, and 16 GB RAM configuration. Pareto front solutions in the 33-bus system obtained for different load characteristic scenarios. In each scenario, the Pareto solution for 4 cases of the study compared to determine the optimal solution from optimal location, number, size, type, and operation of DG and SVC units. The scenarios cases include base case without DG and SVC units, case 1 for optimal solutions of WT units' number, size and location, case 2 for optimal solutions of PV plants number, size and location, case 3 for optimal solutions of combination number of WT and PV units and units size and location, and finally case 4 for optimal solutions of combination number of SVC, WT and PV units and units size and location and SVCs control variables.

The Pareto front solution set of (21) for scenario-1 (residential load curve) shown in Figure 3(a), scenario-2 (industrial load curve) shown in Figure 3(b), scenario-3 (commercial load curve) shown in Figure 3(c) and scenario-4 (real data load curve with mixed load type) shown in Figure 3(d) for different study cases. The solution result obtained by MOSSA for all scenarios shown in the Table 2. The result for scenarios shows that case 4 solutions dominate the Pareto solutions in other cases. In the scenario-1 load curve, except case 2 (installing PV units), all the cases solve voltage violations because the PV plants do not have generated during the nighttime. Total energy losses reduced up to 71.2% in scenario-1, 83.6% in scenario-2, 83.6% in scenario-2, 70.8% in scenario-3 and 80% in scenario-4. The voltage profile comparison for two cases of the base case without DG and SVC units and the case 4 solutions in scenario-4 for peak load hour shown in Figure 4(a).

The same process done for finding different scenarios and study cases Pareto front while satisfying (22) and the voltage profile for the scenario 4 illustrated in Figure 4(b). Different study cases Pareto front for each scenario shown in Figures 5(a) to 5(d) and Table 3 listed the result provided by the obtained Pareto solutions. As shown in Table 3, almost feeders voltage magnitude brings to between 0.95 and 1.05 pu using scenarios study case 1, 3 and 4 and study case2 with installing optimal number, size and site of PV units could not solve voltage violation problem during non-sun irradiation hours. The result shows that for the scenario-1 load curve, the result can reduce the thermal power plant greenhouse gases by 33.8 to 59.4%. The mentioned result for scenario 2 was 26.6 to 60%, for scenario 3 was 32.1 to 59.4%, and for scenario 4 with mixed load data was 40 to 60.1%. Figure 4(b) shows the system's voltage profile for peak load hours (6 PM) in scenario 4.

4.2. 141-bus system

Optimal number, size, location of PV, WT, and SVC units for mixed load curve characteristic to find out best Pareto solutions of minimizing voltage violation, energy losses, thermal generators emission cost, and DG and SVC units' costs. The minimization problems can formulate as (23).

$$\text{Minimize } \{OF_v, OF_l, OF_e, OF_c\}$$
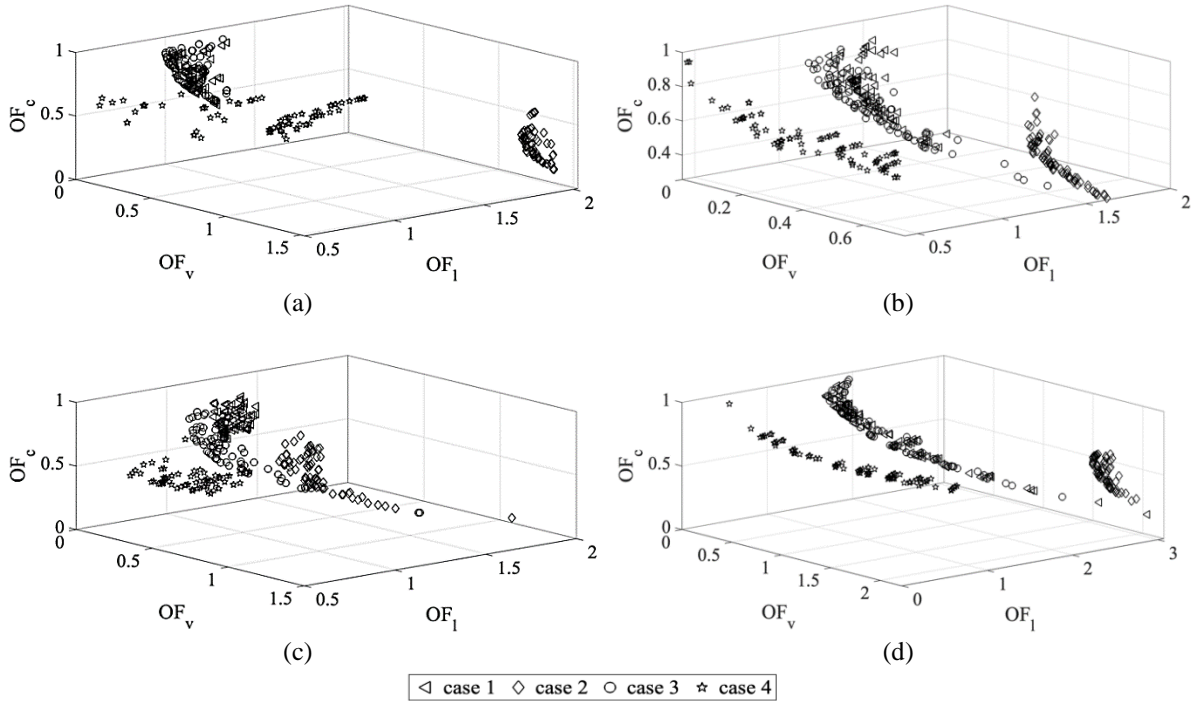$$w.r.t \ \vec{S}, \vec{L}, \vec{O} \tag{23}$$

Figure 3. Pareto front for 33-bus system study for (a) residential load, (b) industrial load, (c) commercial load, and (d) mixed load curve

Table 2. Optimal solution result obtained by MOSSA for (21)

|		DG numbers	SVC numbers			loss at peak hour [kW]		voltage [pu]	
base case							201.8	0.913	1
scenario-1	case 1	5	7			72.0	98.2	0.950	1.031
	case 2	3	7			201.9	201.9	0.913	1.019
	case 3	4	7			71.5	201.9	0.951	1.029
	case 4	1	4	1	5	92.7	775.6	0.952	1.047
scenario-2	case 1	1	7			71.9	584.6	0.950	1.028
	case 2	1	7			64.6	584.6	0.935	1.020
	case 3	1	7			68.4	584.6	0.950	1.041
	case 4	2	6	1	5	21.3	85.3	0.956	1.049
scenario-3	case 1	2	7			66.6	89.6	0.952	1.035
	case 2	2	7			65.1	151.8	0.922	1.037
	case 3	2	7			64.5	123.5	0.950	1.035
	case 4	2	3	2	5	37.7	83.4	0.955	1.070
scenario-4	case 1	2	7			50.4	161.5	0.951	1.018
	case 2	2	7			50.4	152.5	0.914	1.036
	case 3	2	7			50.4	142.8	0.951	1.019
	case 4	1	7	1	5	26.1	126.1	0.950	1.050
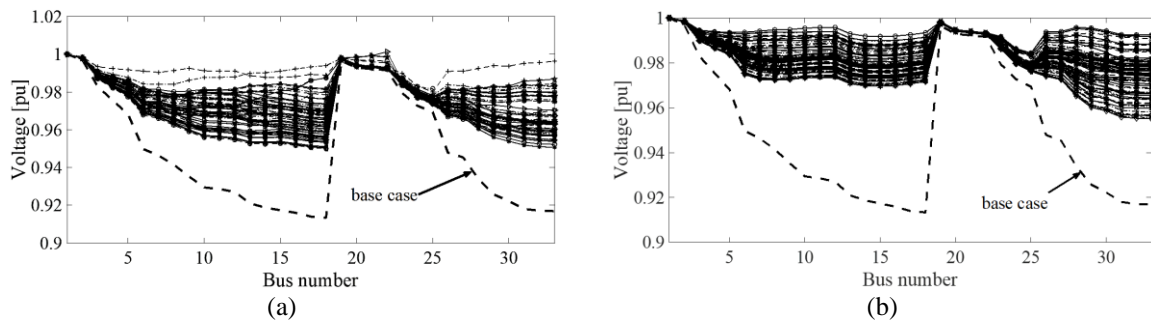
Figure 4. Comparing the voltage profile of case 4 in scenario-4 with the base case for (a) set of (21) objectives and (b) set of (22) objectives
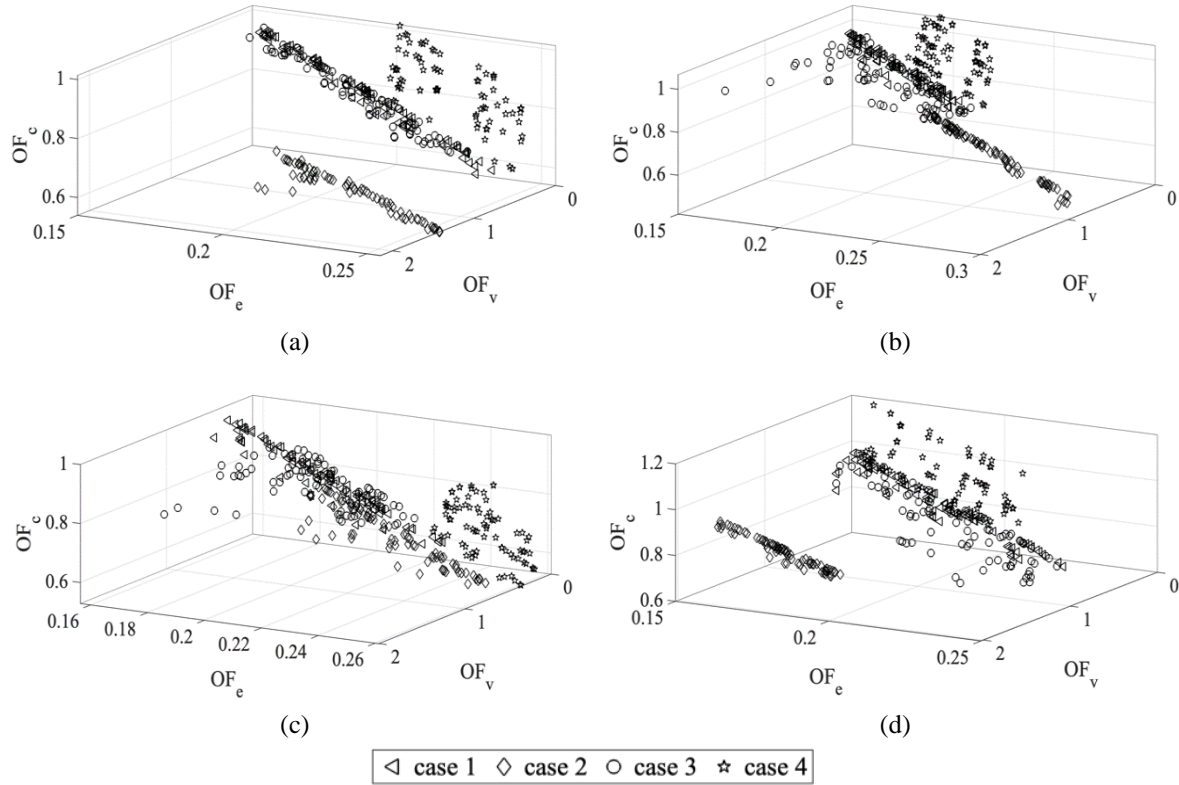
Figure 5. Pareto front for 33-bus system study for (a) residential load, (b) industrial load, (c) commercial load, and (d) mixed load curve

Objective function values for ten optimal Pareto solutions shown in Figure 6. The costs of solutions are is between 1.13 to 1.59 million dollars. Table 4 compares the benefit provided by each Pareto solution with the base case. The result shows that Pareto solutions reduce the total energy losses by 52 to 58% and also reduce the generators emissions between 70.1 to 77.6% compared to the base case. Pareto s9 has the minimum distance to the origin and, compared to other solutions, it has better emissions, energy losses reduction and improving voltage profile. Figure 7 shows the improvement in voltage profile and solving voltage magnitude violation compared to the base case for this solution. The solution includes one PV unit and 12 WT units and 10 SVCs. Figures 8(a) and 8(b) show the solution s3 losses reduction compared to the base case.

Table 3. Optimal solution result obtained by MOSSA for (22)

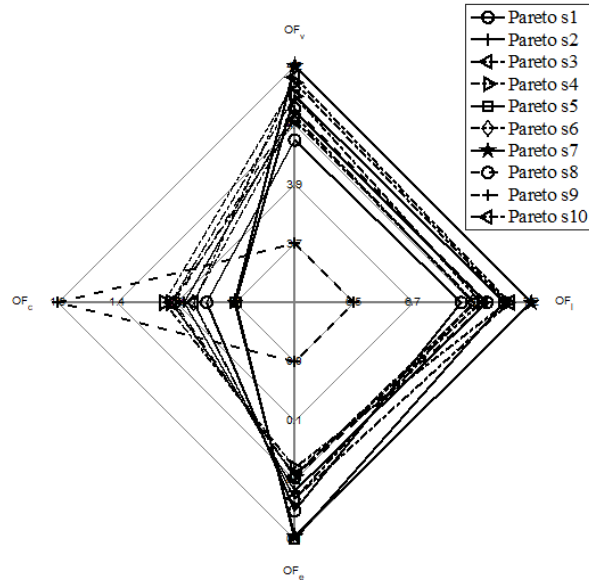|		DG numbers		SVC numbers		loss at peak hour [kW]		voltage [pu]	
base case							201.8	0.913	1
scenario-1	case 1	5	7			72.6	117.3	0.950	1.038
	case 2	5	7			77.8	201.9	0.913	1.050
	case 3	6	7			75.8	138.7	0.951	1.046
	case 4	5	6	1	5	28.3	570.3	0.955	1.033
scenario-2	case 1	5	7			36.6	566.2	0.950	1.032
	case 2	4	7			36.6	566.2	0.933	1.039
	case 3	5	7			59.6	566.2	0.950	1.050
	case 4	6	7	1	5	12.1	78.1	0.951	1.022
scenario-3	case 1	6	7			14.7	111.8	0.950	1.035
	case 2	6	7			14.7	169.9	0.928	1.048
	case 3	6	7			18.8	214.4	0.950	1.050
	case 4	5	7	1	5	18.8	88.6	0.951	1.034
scenario-4	case 1	5	7			18.8	102.7	0.952	1.034
	case 2	5	7			18.8	112.7	0.914	1.047
	case 3	6	7			18.9	112.1	0.951	1.044
	case 4	6	7	1	5	21.8	87.1	0.952	1.022

Figure 6. Pareto front of 141 bus

Table 4. Optimal solution result obtained by MOSSA for (22)

	DG numbers	SVC numbers	Min. voltage [pu]	TEL [MWh]	loss at peak hour [kW]
Pareto s1	10	10	94.7	6.928	402.668
Pareto s2	11	10	94.7	7.035	400.269
Pareto s3	11	10	0.949	6.986	388.955
Pareto s4	13	10	0.950	7.123	387.348
Pareto s5	12	10	0.949	7.112	394.981
Pareto s6	12	10	0.949	6.979	393.946
Pareto s7	11	9	0.948	7.228	409.192
Pareto s8	12	8	0.951	7.038	386.360
Pareto s9	13	10	0.951	6.466	362.065
Pareto s10	11	10	0.950	7.135	391.536
base case			0.928	12.275	628.236
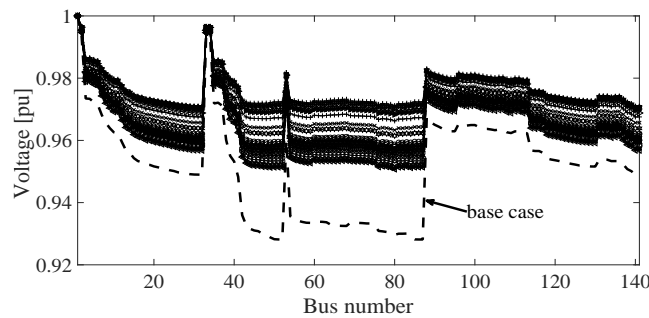
Figure 7. Pareto s9 voltage profile

4.3. Multi-objective algorithm comparison

To analyze the performance and the quality of the MOSSA results, comparisons have been made with MOEA/D and MOPSO for the same condition, parameters, and twenty algorithm runs. Since the Pareto optimal front for the proposed objective function and data is not known to make sure that MOSSA Pareto results are optimal solutions, the algorithms comparisons are based on the C index [36] and spacing metric (S metric) [37], [38].

The S metric is described as the distance of each solution to the closest solution in the search space. Determining a smaller number of the S metric indicates that the archive repository solutions are not distributed evenly. The zero value for this metric corresponds to that all the set solutions are equally spaced. The mathematical formulation for the Spacing metric is shown in (24).

$$S = \sqrt{\frac{1}{k}\sum_{i=1}^{k}(\overline{d} - d_i)^2} \tag{24}$$

where $\overline{d}$ is the average of Euclidean distance. The minimum Euclidean distance for two non-dominated solutions, can be determined as (25) and (26):

$$d_i = \min\left\{\sum_{m=1}^{n}|f_m(x_i) - f_m(x_j)|\right\}, \; j = 1,2,3,\dots,k, j \neq i \tag{25}$$

$$\overline{d} = \frac{1}{k}\sum_{i=1}^{k}d_i \tag{26}$$

The box-plot of the spacing metric for comparing the algorithm shown in Figure 9. The result shows the advantages of MOSSA in finding more evenly distributed solutions. Also, from the result can realize that MOPSO finds the worse spacing metric and the average value for the MOSSA results, the spacing metric calculated as 0.04.

For the C index metric, assume there are A and B as two different sets of Paretos found by different optimization algorithms. The C index for Pareto sets (C(A, B)) represents a number between 0 and 100 and represents the domination percentage of solutions in set B compared to the set A solutions. The definition of the C index can be formulated as (27):

$$C(A, B) := \frac{|\{s_2 \in B; \exists s_1 \in A: s_1 \leq s_2\}|}{|B|} \times 100 \tag{27}$$

where s_1 is one of the solutions in the set A and s_2 is a solution in the Pareto solutions set B.
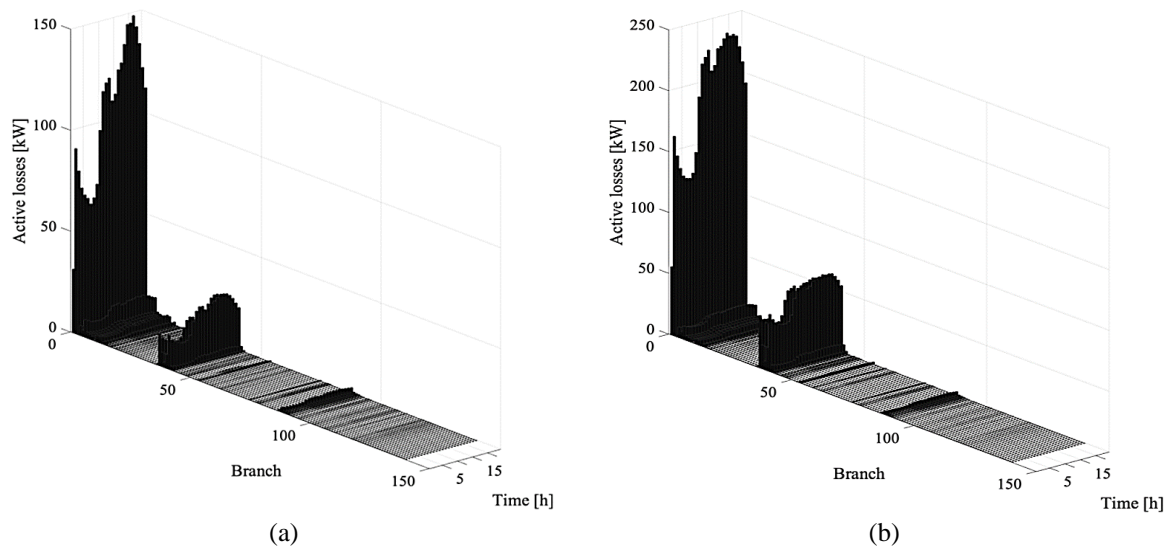

Figure 8. The losses for the system's branches for (a) Pareto s9 and (b) the base case
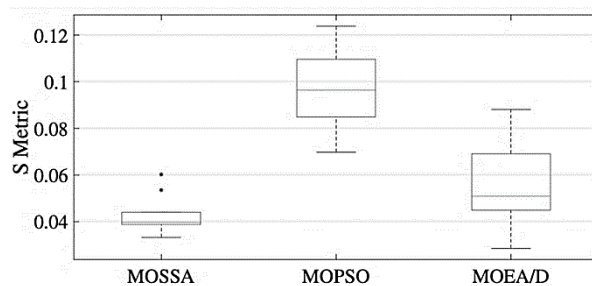

Figure 9. The box-plots of obtained S metrics for MOSSA, MOPSO, and MOEA/D

The box-plot of the C index for comparing algorithm are shown in Figure 10(a) for MOSSA and MOPSO methods and Figure 10(b) for MOSSA and MOEA/D algorithms. The result shows that the MOPSO and MOEA/D solutions dominated by the MOSSA solution up to 60% while this amount for dominating the solution of MOSSA by MOPSO and MOEA/D is less than 10%. The result shows that the MOSSA has outstanding searching performance, and the quality and performance of the Pareto front solution are better than two other algorithms.
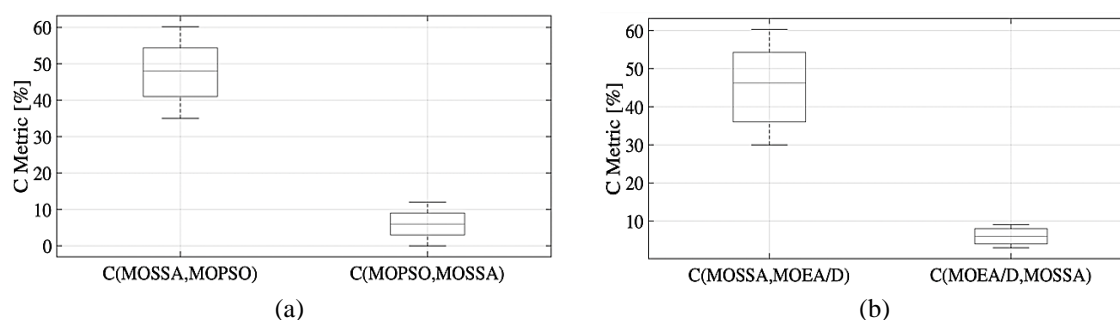

Figure 10. C index box-plot for comparing algorithms (a) C index comparison to MOPSO and (b) C index comparison to MOEA/D

5. CONCLUSION

In this work, a novel approach based on MOSSA has been presented and applied to find the Pareto optimal solutions for various problems in the distribution system. For this purpose, the optimal location, size, and type of DG units and also the optimal location and size and the operation strategy of the small-scaled SVCs were determined concerning the different objective functions. The problems were formulated as a multi-objective optimization problem, consideration of minimum DGs and SVC cost, minimum voltage violation, minimum energy losses and minimum system emission cost for different load characteristics. For the 33-bus test system, the Pareto front solutions of different scenarios for the characteristic of the load and different assumptions for DG type were found for two different sets of objective functions. All the obtained benefits, such as improvement in the voltage profile and the reduction of the line losses discussed, and the best number of DG and SVC units, were found by comparing the results. In the 141-bus system for a mixed load curve and a set of all objective functions, the Pareto solutions determine, and for 10 obtained Pareto solutions, all the benefits provided by the solutions compared with the base case. Finally, the MOSSA Pareto solution quality and performance compared to the results of MOEA/D and MOPSO algorithms. As the conclusion of the result, it is evident that the MOSSA result can be accepted as the near-optimal Pareto solution. In addition, the optimal allocation parameters of the DG and SVC units and also operation strategy of the units can be used in the real distribution system for different load conditions and DG units' output.

REFERENCES

[1] M. Aryanezhad, "Optimization of grid connected bidirectional V2G charger based on multi-objective algorithm," in *2017 8th Power Electronics, Drive Systems and Technologies Conference (PEDSTC)*, 2017, pp. 519–524, doi: 10.1109/PEDSTC.2017.7910381.

[2] M. Aryanezhad, M. Joorabian, and E. Ostadaghaee, "A novel simplified approach to complexity of power system components including nonlinear controllers based model reduction," *International Journal of Electrical Power and Energy Systems*, vol. 73, pp. 298–308, Dec. 2015, doi: 10.1016/j.ijepes.2015.05.013.

[3] S. R. Salkuti, "Optimal reactive power scheduling using cuckoo search algorithm," *International Journal of Electrical and Computer Engineering (IJECE)*, vol. 7, no. 5, pp. 2349–2356, Oct. 2017, doi: 10.11591/ijece.v7i5.pp2349-2356.

[4] M. Lakshmi, and A. Ramesh Kumar, "Optimal reactive power dispatch using crow search algorithm," *International Journal of Electrical and Computer Engineering (IJECE)*, vol. 8, no. 3, pp. 1423–1431, Jun. 2018, doi: 10.11591/ijece.v8i3.pp1423-1431.

[5] M. Aryanezhad, E. Ostadaghaee, and M. Joorabian, "Optimal allocation and sizing of FACTS devices based non-dominated sorting genetic algorithm II," *The 1st Iran Energy Association National Conference-2013 Tehran*, 2013.

[6] B. Ahmadi, O. Ceylan, and A. Ozdemir, "Impacts of load and generation volatilities on the voltage profiles improved by distributed energy resources," in *2020 55th International Universities Power Engineering Conference (UPEC)*, Sep. 2020, pp. 1–6, doi: 10.1109/UPEC49904.2020.9209811.

[7] H. Han *et al.*, "Optimal sizing considering power uncertainty and power supply reliability based on LSTM and MOPSO for SWPBMs," *IEEE Systems Journal*, pp. 1–11, 2022, doi: 10.1109/JSYST.2021.3137856.

[8] V. M. Jyothi, T. V. Muni, and S. V. N. L. Lalitha, "An optimal energy management system for PV/battery standalone system," *International Journal of Electrical and Computer Engineering (IJECE)*, vol. 6, no. 6, pp. 2538–2544, Dec. 2016, doi: 10.11591/ijece.v6i6.pp2538-2544.

[9] D. Singh, D. Singh, and K. S. Verma, "Ga based optimal sizing and placement of distributed generation for loss minimization,"

International Journal of Electrical and Computer Engineering (IJECE), vol. 2, no. 8, pp. 556–562, 2007.

[10]　E. kianmehr, S. Nikkhah, and A. Rabiee, "Multi-objective stochastic model for joint optimal allocation of DG units and network reconfiguration from DG owner's and DisCo's perspectives," *Renewable Energy*, vol. 132, pp. 471–485, Mar. 2019, doi: 10.1016/j.renene.2018.08.032.

[11]　P. G. Burade, "Optimal location of FACTS device on enhancing system security," *International Journal of Electrical and Computer Engineering (IJECE)*, vol. 2, no. 3, pp. 309–316, Apr. 2012, doi: 10.11591/ijece.v2i3.250.

[12]　S. Arabi Nowdeh *et al.*, "Fuzzy multi-objective placement of renewable energy sources in distribution system with objective of loss reduction and reliability improvement using a novel hybrid method," *Applied Soft Computing*, vol. 77, pp. 761–779, Apr. 2019, doi: 10.1016/j.asoc.2019.02.003.

[13]　M. Ghiasi, "Detailed study, multi-objective optimization, and design of an AC-DC smart microgrid with hybrid renewable energy resources," *Energy*, vol. 169, pp. 496–507, Feb. 2019, doi: 10.1016/j.energy.2018.12.083.

[14]　S. Xie, Z. Hu, and J. Wang, "Two-stage robust optimization for expansion planning of active distribution systems coupled with urban transportation networks," *Applied Energy*, vol. 261, Mar. 2020, doi: 10.1016/j.apenergy.2019.114412.

[15]　S. Sultana and P. K. Roy, "Krill herd algorithm for optimal location of distributed generator in radial distribution system," *Applied Soft Computing*, vol. 40, pp. 391–404, Mar. 2016, doi: 10.1016/j.asoc.2015.11.036.

[16]　S. Kumar, K. K. Mandal, and N. Chakraborty, "Optimal DG placement by multi-objective opposition based chaotic differential evolution for techno-economic analysis," *Applied Soft Computing*, vol. 78, pp. 70–83, May 2019, doi: 10.1016/j.asoc.2019.02.013.

[17]　S. M. Faresse, M. Assini, and A. Saad, "Hybrid energy storage system optimal sizing for urban electrical bus regarding battery thermal behavior," *International Journal of Electrical and Computer Engineering (IJECE)*, vol. 10, no. 3, pp. 2894–2911, Jun. 2020, doi: 10.11591/ijece.v10i3.pp2894-2911.

[18]　B. Ahmadi, O. Ceylan, and A. Ozdemir, "Optimal allocation of multi-type distributed generators for minimization of power losses in distribution systems," in *2019 20th International Conference on Intelligent System Application to Power Systems (ISAP)*, Dec. 2019, pp. 1–6, doi: 10.1109/ISAP48318.2019.9065974.

[19]　N. M. Ahmed, H. M. Farghally, and F. H. Fahmy, "Optimal sizing and economical analysis of PV-wind hybrid power system for water irrigation using genetic algorithm," *International Journal of Electrical and Computer Engineering (IJECE)*, vol. 7, no. 4, pp. 1797–1814, Aug. 2017, doi: 10.11591/ijece.v7i4.pp1797-1814.

[20]　M. N. Dazahra, F. Elmariami, A. Belfqih, and J. Boukherouaa, "Optimal location of SVC using particle swarm optimization and voltage stability indexes," *International Journal of Electrical and Computer Engineering (IJECE)*, vol. 6, no. 6, pp. 2581–2588, Dec. 2016, doi: 10.11591/ijece.v6i6.pp2581-2588.

[21]　S. M. Safdarnejad, J. F. Tuttle, and K. M. Powell, "Dynamic modeling and optimization of a coal-fired utility boiler to forecast and minimize NOx and CO emissions simultaneously," *Computers and Chemical Engineering*, vol. 124, pp. 62–79, May 2019, doi: 10.1016/j.compchemeng.2019.02.001.

[22]　Y. Censor, "Pareto optimality in multiobjective problems," *Applied Mathematics and Optimization*, vol. 4, no. 1, pp. 41–59, Mar. 1977.

[23]　S. Mirjalili, A. H. Gandomi, S. Z. Mirjalili, S. Saremi, H. Faris, and S. M. Mirjalili, "Salp swarm algorithm: a bio-inspired optimizer for engineering design problems," *Advances in Engineering Software*, vol. 114, pp. 163–191, Dec. 2017, doi: 10.1016/j.advengsoft.2017.07.002.

[24]　A. A. Alabduljabbar and J. V Milanović, "Assessment of techno-economic contribution of FACTS devices to power system operation," *Electric Power Systems Research*, vol. 80, no. 10, pp. 1247–1255, Oct. 2010, doi: 10.1016/j.epsr.2010.04.008.

[25]　K. Mongird *et al.*, "Energy storage technology and cost characterization report," Richland, WA (United States), Jul. 2019. doi: 10.2172/1573487.

[26]　R. Fu, D. J. Feldman, and R. M. Margolis, "U.S. solar photovoltaic system cost Benchmark: Q1 2018," Nov. 2018, doi: 10.2172/1483475.

[27]　R. Wiser and M. Bolinger, "2018 Wind technologies market report," Department of Energy, United State, Aug. 2019. doi: 10.2172/1559881.

[28]　K. Liu, W. Sheng, Y. Liu, X. Meng, and Y. Liu, "Optimal sitting and sizing of DGs in distribution system considering time sequence characteristics of loads and DGs," *International Journal of Electrical Power and Energy Systems*, vol. 69, pp. 430–440, Jul. 2015, doi: 10.1016/j.ijepes.2015.01.033.

[29]　M. E. Baran and F. F. Wu, "Network reconfiguration in distribution systems for loss reduction and load balancing," *IEEE Transactions on Power Delivery*, vol. 4, no. 2, pp. 1401–1407, Apr. 1989, doi: 10.1109/61.25627.

[30]　H. M. Khodr, F. G. Olsina, P. M. D. O.-D. Jesus, and J. M. Yusta, "Maximum savings approach for location and sizing of capacitors in distribution systems," *Electric Power Systems Research*, vol. 78, no. 7, pp. 1192–1203, Jul. 2008, doi: 10.1016/j.epsr.2007.10.002.

[31]　U. Eminoglu and M. H. Hocaoglu, "Distribution systems forward/backward sweep-based power flow algorithms: a review and comparison study," *Electric Power Components and Systems*, vol. 37, no. 1, pp. 91–110, Dec. 2008, doi: 10.1080/15325000802322046.

[32]　C. Yammani, S. Maheswarapu, and S. K. Matam, "A multi-objective shuffled Bat algorithm for optimal placement and sizing of multi distributed generations with different load models," *International Journal of Electrical Power and Energy Systems*, vol. 79, pp. 120–131, Jul. 2016, doi: 10.1016/j.ijepes.2016.01.003.

[33]　B. Ahmadi, S. Younesi, O. Ceylan, and A. Ozdemir, "An advanced grey wolf optimization algorithm and its application to planning problem in smart grids," *Soft Computing*, Feb. 2022, doi: 10.1007/s00500-022-06767-9.

[34]　S. Pfenninger and I. Staffell, "Long-term patterns of European PV output using 30 years of validated hourly reanalysis and satellite data," *Energy*, vol. 114, pp. 1251–1265, Nov. 2016, doi: 10.1016/j.energy.2016.08.060.

[35]　I. Staffell and S. Pfenninger, "Using bias-corrected reanalysis to simulate current and future wind power output," *Energy*, vol. 114, pp. 1224–1239, Nov. 2016, doi: 10.1016/j.energy.2016.08.068.

[36]　E. Zitzler, K. Deb, and L. Thiele, "Comparison of multiobjective evolutionary algorithms: empirical results," *Evolutionary Computation*, vol. 8, no. 2, pp. 173–195, 2000.

[37]　J. R. Schott, "Fault tolerant design using single and multicriteria genetic algorithm optimization," Thesis (M.S.)--Massachusetts Institute of Technology, Dept. of Aeronautics and Astronautics, 1995.

[38]　B. Ahmadi, O. Ceylan, and A. Ozdemir, "A multi-objective optimization evaluation framework for integration of distributed energy resources," *Journal of Energy Storage*, vol. 41, Sep. 2021, doi: 10.1016/j.est.2021.103005.

BIOGRAPHIES OF AUTHORS

Bahman Ahmadi 🆔 📇 SC Ⓟ received his BSc degree in Electrical engineering from Urmia University, Urmia, Iran in 2017. He is currently a master student in Istanbul Technical University, Istanbul, Turkey. His current research interests include Meta-heuristics optimization algorithm and smart grid. He can be contacted at email: ahmadi18@itu.edu.tr.

Ramazan Çağlar 🆔 📇 SC Ⓟ is an Assoc. Professor in the Faculty of Electrical and Electronics Engineering at the Istanbul Technical University where he has been a faculty member since 2004. He completed his Ph.D. at the same University in 1999. He was the Postdoctoral Researcher in the School of Electric and Computer Engineering at Georgia Institute of Technology, Atlanta, USA between 2001 and 2003. His research interest are modeling, analysis, and control of power system, reliability analysis, electricity market, smart grids, renewable generations, fault diagnosis, risk management and signal processing. Dr. Çağlar is a member of IEEE, IEEE-PES, a member of CIGRE, and a member of Turkish National Committee on Illumination (ATMK). He can be contacted at email: caglarr@itu.edu.tr.